

Title: Cortical selectivity driven by connectivity: Innate connectivity patterns of the visual word form area

Authors: Jin Li, David E. Osher, Heather A. Hansen, Zeynep M. Saygin

Affiliation: Department of Psychology & Center for Cognitive and Brain Sciences, The Ohio State University

Please address correspondence to:

Jin Li, Department of Psychology, The Ohio State University, 225 Psychology Building, 1835 Neil Avenue, Columbus, OH, 43210. E-mail: li.9361@osu.edu

and

Zeynep M. Saygin, Department of Psychology, The Ohio State University, 225 Psychology Building, 1835 Neil Avenue, Columbus, OH, 43210. E-mail: saygin.3@osu.edu

18

19

Abstract

20 The human brain is a patchwork of different functionally specialized areas. What
21 determines this functional organization of cortex? One hypothesis is that innate
22 connectivity patterns shape functional organization by setting up a scaffold upon which
23 functional specialization can later take place. We tested this hypothesis here by asking
24 whether the visual word form area (VWFA), an experience-driven region that only
25 becomes selective to visual words after gaining literacy, was already connected to proto
26 language networks in neonates scanned within one week of birth. We found that
27 neonates showed adult-like functional connectivity, and observed that i) the VWFA
28 connected more strongly with frontal and temporal language regions than regions
29 adjacent to these language regions (e.g., frontal attentional demand, temporal auditory
30 regions), and ii) language regions connected more strongly with the putative VWFA than
31 other adjacent ventral visual regions that also show foveal bias (e.g. fusiform face area,
32 FFA). Object regions showed similar connectivity with language areas as the VWFA but
33 not with face areas in neonates, arguing against prior hypotheses that the region that
34 becomes the VWFA starts out with a selectivity for faces. These data suggest that the
35 location of the VWFA is earmarked at birth due to its connectivity with the language
36 network, providing novel evidence that innate connectivity instructs the later refinement
37 of cortex.

INTRODUCTION

Decades of research suggest that the adult brain is composed of patches of cortex that are specialized for unique mental functions. To what extent is the functional organization of the human brain innate? Recent advances in developmental neuroimaging have made it possible to start to answer this question. For example, a recent study showed category-selective responses in high-level visual cortex for faces and scenes in infants¹. Moreover, research in congenitally blind individuals suggests that cortical selectivity for high-level visual categories may not require visual experience². In addition to the early emergence of visual processing, a previous study also found a neural precursor of language processing in infants³. Specifically, they found brain activity in left superior temporal and angular gyri to human speech in 3-month-old infants. These studies support the protomap hypothesis, which suggests that early genetic instructions give rise to the mature functional areas of the cortex.

However, the driving factor of this early functional specialization remains ambiguous.

The Connectivity Hypothesis proposes that the specialization of a given brain region is largely shaped by how it connects and communicates with the rest of the brain.

Alternative (but not mutually exclusive) hypotheses are that the location of a given brain region is determined by its intrinsic molecular or circuit properties or, in the case of visual areas, by pre-existing featural or retinotopic biases that predispose a region to become selective to foveal or peripheral stimuli (Retinotopic Hypothesis)⁴⁻⁷. Previous work showed that structural connectivity (via diffusion imaging) can predict the functional selectivity of a brain region to different visual categories (i.e., faces, scenes, objects, bodies)^{8, 9}. Functional connectivity (FC) (through resting-state scans) can also

61 be used to predict selectivity to various functional selectivity across the brain¹⁰⁻¹². This
62 work suggests that, at least in adults, connectivity is tightly intertwined with functional
63 selectivity.

64 Few studies have examined whether early connectivity patterns may earmark cortical
65 tissue as the future site of a functionally specific region. A resting-state FC study in
66 macaques found that while newborn macaques deprived of faces did not show face-
67 selective responses, they did show a proto-organization for retinotopy throughout the
68 visual system¹³. This study supports the Connectivity Hypothesis as well as the
69 Retinotopic Hypothesis, by suggesting that connectivity with early visual areas may set
70 up a retinotopic scaffold upon which early viewing behavior, paired with the right type of
71 input (e.g. faces) may then bias domain formation in stereotyped locations in high-level
72 visual cortex. However, there likewise exists highly experience-dependent visual
73 regions that are also in stereotyped locations, like the visual word form area (VWFA),
74 which responds strongly to visual words or letter strings and only exists in literate
75 individuals^{14, 15}. How does the VWFA differentiate from the adjacent fusiform face area
76 (FFA)? The perception of both words and faces requires the analysis of high-spatial
77 frequency and foveal input¹⁶⁻¹⁸, and thus connectivity to early retinotopic areas may not
78 differentiate them. Alternatively, the VWFA may become increasingly selective to visual
79 words and may be differentiated from FFA by communicating with other regions, e.g.
80 the language network. Thus, contrasting the development of the VWFA vs. FFA will help
81 disentangle the Connectivity Hypothesis from the Retinotopic Hypothesis.

82 In adults, the VWFA connects with perisylvian language cortex, differentiating it
83 from adjacent visual cortex¹⁹; other studies also found that white matter fibers that

originated from the VWFA pass through fascicles that may be critical for language processing^{20, 21}. In children, a longitudinal study found that connectivity patterns in pre-literate 5-year-olds predicted the location of the VWFA in each child at age 8 after they learned to read, and differentiated it from the adjacent FFA²². The connectivity patterns that predicted the VWFA included putative language areas, suggesting that connectivity to these regions may earmark the future location of a visual region that is selective to words, and also set up a scaffold upon which future functional specialization can take place. However, while the 5-year-olds could not read (and at that age, lacked neural selectivity to letters or letter-like stimuli), they still would have had years of visual experience with letters and words. Is the putative VWFA already connected differently and set up to be differentiated from adjacent visual regions, even at birth? Alternatively, is the VWFA recycled from the adjacent FFA⁷ or other adjacent regions; in other words, is the VWFA undifferentiated from the FFA in terms of its connectivity to language areas in neonates?

Here, we tested this proto-organization of the VWFA in the newborn brain. Based on the Connectivity Hypothesis, we hypothesized that although the VWFA is highly experience-dependent, it is already 'prewired' to be selective for visual words by communicating with proto language regions at birth. Specifically, by examining neonates who were scanned within one week of birth, we asked i) Does the VWFA show adult-like FC with the temporal and inferior frontal language network compared with adjacent regions like the multiple-demand (MD) network, speech regions, and primary auditory cortex (A1)? ii) Are connections stronger between language areas and

the cortical tissue of the putative VWFA, than with other visual areas within the ventral temporal cortex?

RESULTS

FC between the putative VWFA and language regions

We examined whether the putative VWFA already showed adult-like FC patterns even at birth. First, we asked, does this cortical tissue connect more to language regions vs. regions in the vicinity of language areas? We identified the putative VWFA, frontal and temporal language regions; as a comparison, we also included frontal multiple-demand (MD) regions (which activate during a wide variety of cognitively demanding tasks), speech regions in perisylvian cortex that don't respond preferentially to language but rather more generally to human speech sounds (much like a higher order auditory cortex), and primary auditory cortex (A1) (see Online Methods; **Fig. 1a**). The regions were defined in independent groups of adults and overlaid on the individual anatomical space of neonates and adults in this dataset (see Online Methods).

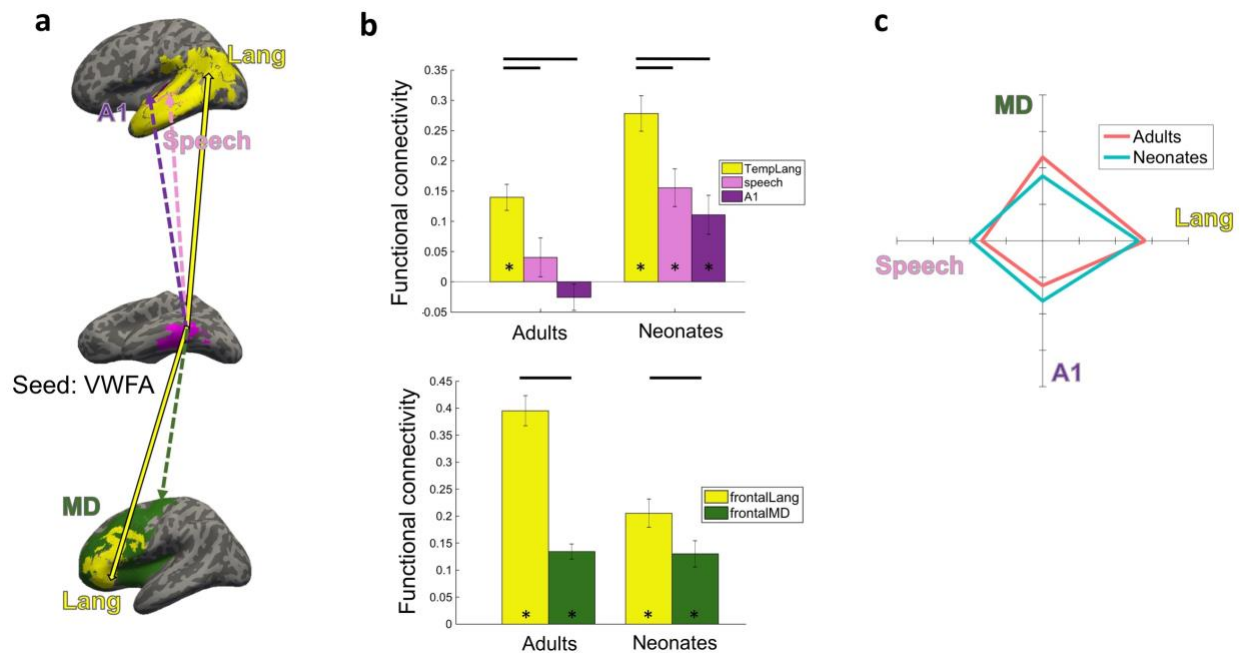


Figure 1 FC between VWFA (seed) and non-visual regions (targets). **(a)** Functional parcels overlaid on an example inflated brain and a schema of the connectivity analysis: VWFA (magenta), language (yellow), speech (pink), A1 (purple), MD (dark green). **(b)** Top, mean FC between VWFA and regions in temporal cortex. Bottom, mean FC between VWFA and frontal language regions and MD regions. Connectivity values were Fisher z transformed. Error bars denote s.e.m. Horizontal bars reflect significant *post hoc* paired *t*-tests $p < 0.05$, corrected. **(c)**: FC fingerprint of VWFA. Connectivity values were mean-centered and averaged within each of the four categories to plot the relative patterns for the adult and neonate groups. TempLang, temporal language regions; frontalLang, frontal language regions; frontalMD, frontal multiple-demand regions. * denotes significant one-sample *t*-test ($p < 0.05$).

We calculated the functional connectivity (FC) between the VWFA (seed region) and the language, MD, speech, and A1 regions (target regions). First, we examined the VWFA's connectivity to temporal regions. We ran a 2-way ANOVA of age group (neonate, adult) \times target (temporal language regions, speech, A1) and found significant main effects for both target and age group (target: $F(2,225) = 17.23$, $p < 0.001$; age group: $F(1,225) = 30.51$, $p < 0.001$), and no interaction between age group and target.

Both adults and neonates showed higher connectivity between the VWFA and language parcels compared with the connectivity between the VWFA and the adjacent speech region (**Fig. 1b**, top; *post-hoc t*-tests: adult: $t(74) = 2.54$, $p < 0.05$, corrected, 95% confidence interval (CI) = [0.02, 0.18]; neonate: $t(76) = 2.83$, $p < 0.05$, corrected; 95% CI = [0.04, 0.21]) and A1 (adult: $t(74) = 5.29$, $p < 0.001$, corrected, 95% CI = [0.10, 0.23]; neonate: $t(76) = 3.79$, $p < 0.001$, corrected, 95% CI = [0.08, 0.26]).

Next, since language regions also exist in frontal cortex, we explored the connectivity of the VWFA to frontal language regions. To control for potential distance or location confounds, we compared the connectivity between the VWFA to frontal language regions vs. the connectivity between the VWFA to frontal multiple-demand (MD) regions, which are intertwined with language regions but are functionally distinct from them (**Fig. 1a**). We first ran a 2-way ANOVA of age group (neonate, adult) \times target (frontal language, frontal MD) and found significant main effects for both target and age group (target: $F(1,150) = 48.72$, $p < 0.001$; age group: $F(1,150) = 16.29$, $p < 0.001$), and the interaction between target and age group was also significant ($F(1,150) = 14.85$, $p < 0.001$). We found that the connectivity between the VWFA to frontal language regions was significantly higher than its connectivity to frontal MD regions (adult: $t(74) = 8.23$, $p < 0.001$, corrected, 95% CI = [0.20, 0.32]; neonate: $t(76) = 2.08$, $p < 0.05$, corrected, 95% CI = [0, 0.15]) (**Fig. 1b**, bottom). These findings are summarized by the connectivity fingerprint plot in **Fig. 1c**, which indicates similar shapes (i.e., similar connectivity patterns) between neonates and adults. These results indicate that the cortical tissue that will later develop sensitivity to visual words have connectivity patterns that are relatively adult-like in the neonatal brain, suggesting that it is

earmarked to become functionally specialized by showing preferential connectivity with language regions at birth.

The selectivity of VWFA-language connections compared with other visual areas

Next, we asked: do language regions selectively connect to the expected site of the VWFA, compared with other adjacent high-level visual regions? To answer this question, we compared the connectivity of language regions to the VWFA vs. connectivity of language regions to other high-level visual areas in the ventral stream, specifically in regions in the vicinity of the VWFA, including face selective regions (Fusiform Face Area, FFA; Occipital Face Area, OFA), scene selective region (Parahippocampal Place Area; PPA), and object selective regions (Lateral Occipital, LO; Posterior Fusiform Sulcus, PFS) (**Fig. 2a**). These regions were overlaid on the individual anatomical space as above (see Online Methods).

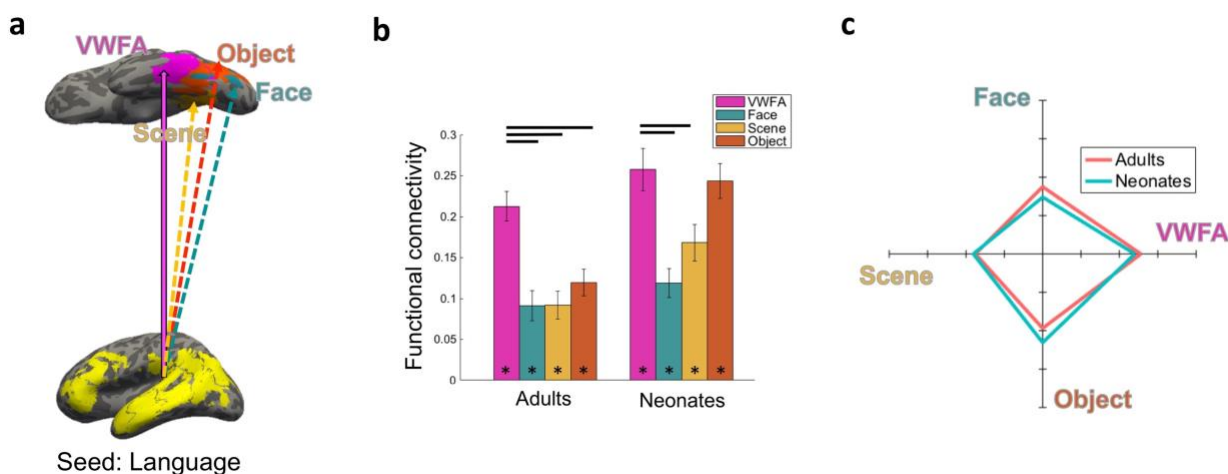


Figure 2 FC between language regions (seed) and high-level visual regions (targets). **(a)** Functional parcels and a schema of the connectivity analysis: language (yellow), VWFA (magenta), faces (blue), scenes (gold), objects (orange) **(b)** Mean FC between language regions and high-level visual regions in ventral visual stream. Connectivity

values were Fisher z transformed. Error bars denote s.e.m. Horizontal bars reflect significant *post hoc* paired *t*-tests $p < 0.05$, corrected. (c): FC fingerprint of language regions. Connectivity values were mean-centered and averaged within each of the four categories to plot the relative patterns for the adult and neonate groups. * denotes significant one-sample *t*-test ($p < 0.05$).

We ran a 2-way ANOVA of age group (neonate, adult) \times target (VWFA, faces, scenes, objects) and found significant main effects for both target and age group (target, $F(3,300) = 16.32$, $p < 0.001$; age group, $F(1,300) = 22.88$, $p < 0.001$; marginal significant interaction between target and age group ($F(3,300) = 2.19$, $p = 0.089$). *Post-hoc t*-tests revealed that in adults, the connectivity between language regions and the VWFA was significantly higher than all other high-level visual regions tested (face: $t(74) = 4.64$, $p < 0.001$, corrected, 95% CI = [0.07, 0.17]; scene: $t(74) = 4.80$, $p < 0.001$, corrected, 95% CI = [0.07, 0.17]; object: $t(74) = 3.80$, $p < 0.001$, corrected, 95% CI = [0.04, 0.14]) (**Fig. 2b**). The neonates showed a similar pattern, where connectivity between language regions and the VWFA was significantly higher than connectivity of language regions to face ($t(76) = 4.39$, $p < 0.001$, corrected; scene, 95% CI = [0.08, 0.20]; $t(76) = 2.58$, $p < 0.05$, corrected, 95% CI = [0.02, 0.16]), but no difference between language regions' connectivity to the VWFA vs. object regions in neonates (**Fig. 2b**). These results indicate that neonates show an overall similar FC pattern as adults (**Fig. 2c**), with highest connectivity between language regions and VWFA; however, given that neonates show similar connectivity between language-VWFA and language-object regions, it suggests that there is further developmental refinement as functional specialization takes place.

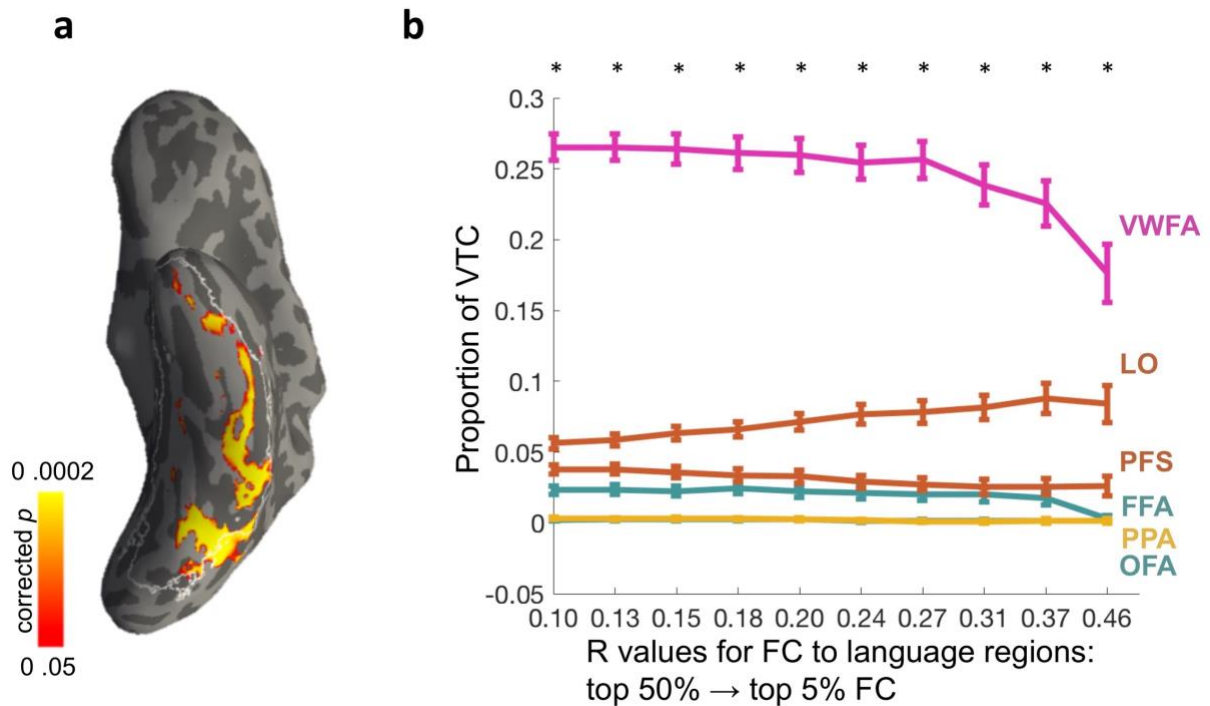


Figure 3 Voxel-wise analysis using language regions as the seed and each voxel within the ventral temporal cortex (VTC) as a target in the neonatal group. **(a)** Heatmap of voxels within VTC that are significantly connected with language regions (FWE-corrected by nonparametric permutation tests) and overlaid on an example brain. The white line denotes the VTC search space. **(b)** The proportion of VTC voxels that connect with language regions at increasing FC strengths, from the median to the top 95th percentile, are plotted for each VTC region. Error bars denote s.e.m across participants. * denotes significant paired t -test (VWFA vs. averaged of other functional regions, $p < 0.05$, corrected).

Next, to get a finer characterization of the connectivity between language regions and the whole ventral temporal cortex (VTC) in neonates, we performed a voxel-wise analysis within the VTC to explore which voxels connect most with language regions. One-sample t -tests were performed across neonates to identify voxels that are significantly connectivity with language regions (FWE corrected by nonparametric permutation tests, $p < 0.05$)²³; these voxels were located mostly in the lateral fusiform

gyrus and a more posterior part of VTC (**Fig. 3a**). To identify which functional regions these voxels belonged to, we parametrically increased a threshold from the median to the top 95th percentile of FC across the VTC, and calculated the number of voxels within the VTC that were connected to language regions; we then quantified how many of these voxels belonged in each functional region (as a proportion of all VTC voxels that passed the threshold; Online Methods). We found that voxels that were connected to language regions were always located in the expected site of VWFA, above and beyond all other functional regions in the vicinity; this result was significant for all thresholds (**Fig. 3b**). We additionally did the same voxel-wise analysis in adult group, and again found that highest proportion of VTC voxels were located in VWFA compared with other adjacent high-level visual regions, which were significant for all threshold from the median to the top 95th percentile of FC.

Discussion

A mosaic-like functional organization is consistently found in the adult brain. However, the driving factor of this functional organization and its variation across individuals remains unclear. The Connectivity Hypothesis proposes that the future function of a given brain area is largely shaped by how this region connects with the rest of the brain. Other alternative accounts (that are not mutually exclusive with the Connectivity Hypothesis) are that other factors, such as retinotopic biases (i.e. Retinotopic Hypothesis) or other intrinsic cellular specialization, may set up a protomap for functional organization. Classic studies of 'rewired' ferrets showed that the cortical

region that would have developed into A1 took on many of the properties of V1 after retinal input was rerouted to that location, showing in animal models that connectivity precedes function²⁴⁻²⁸. Our findings extend this work from primary sensory cortex to high-level cortical regions in human neonates. In the present study, we investigated the connectivity patterns of the putative VWFA, a highly experience-dependent region, in the neonatal brain, and asked: is this region already pre-wired at birth to develop differential functional specialization from its neighbors? We found that the putative VWFA already shows adult-like connectivity patterns in neonates. Specifically, this cortical tissue may be earmarked to become selective to visual words by showing preferential connectivity with language regions. Moreover, the present study indicates that despite the early development of high-level visual cortex¹, language regions specifically connect with the future site of VWFA compared with adjacent face and scene regions, just like adults. This research provides the earliest possible evidence in humans that the cortical tissue that will later develop sensitivity to visual words has a connectivity pattern at birth that makes it fertile-ground for such development – even before any exposure to words.

A recent study found that the VWFA has preferential FC with the core language system in adults²⁹. Our study replicates this FC pattern, but importantly, we find that the preferential FC (and structural connectivity) between VWFA and language regions already exists in the neonatal brain. This result suggests that although neonates might not have a VWFA, this cortical tissue is already set up for its future function by showing higher connectivity with putative language regions. This provides strong evidence for the Connectivity Hypothesis of the functional organization of our brain. Moreover, our

results indicate that there is little, if any, communication between the VWFA and either A1 or the adjacent speech region, which is sensitive to the features of human speech (i.e., segmental and suprasegmental phonological properties). Infants within the first month of life show neural activation for speech vs. backwards speech³. Our results suggest that VWFA does not show preferential functional or structural connectivity with speech-selective regions in adults, but rather with adjacent language regions that are selective to higher-level semantic properties; further we show that this organization is present even at birth. These results suggest that the connectivity patterns of the putative VWFA are spatially precise even in newborns, and that phonemic representations for visual words may be accessed through other networks.

The VWFA serves as a good model to study the emergence of functionally selective regions. This region is highly experience-dependent and so it is almost certainly selective or shows preferential visual responses to another stimulus type (e.g., recycled from another high-level region) before the experience is gained. Previous studies posited that this cortical tissue starts out as part of the face network, and becomes increasingly selective to words and less selective to faces in the left hemisphere as literacy is acquired^{15, 30}. This hypothesis is an attractive one because the perception of both faces and words require high-spatial frequency information that is represented foveally. Thus, with a retinotopic bias/connectivity from lower-level visual regions, it may be possible to first differentiate face regions from scene regions (foveal vs. peripheral bias) early in development (if not at birth), and then face from word regions after literacy is gained, perhaps through differential connections with fronto-temporal language regions. In contrast, our study finds evidence that the VWFA is in fact similar in its

connectivity with language regions as object regions, suggesting that the putative VWFA may first be undifferentiated from object regions. This result aligns with another study which found that young children's letter-recognition abilities may be related to their object recognition skills³¹. Moreover, a recent study shows that although the VWFA can be defined with words vs. faces in both skilled and struggling readers, the VWFA in struggling readers shows similar selectivity to words as it does to objects³². One possibility is that while the VWFA is already differentiated from face and scene areas at birth, it gains its selectivity to orthography through relevant experience and splits off from object cortex through repeated co-activations and further strengthening of its connections with language cortex. This hypothesis should be tested longitudinally to see how connections are strengthened and/or weakened as an individual gains literacy and as this piece of cortex begins to show preferential responses to orthography.

Another question that is raised by the present study is how the connectivity patterns themselves arose prenatally and evolutionarily. It is likely that a complex mechanism of intrinsic cellular or properties in different cortical regions and early signaling mechanisms set up these large-scale connections. It is possible that the VWFA is simply in a privileged location, due to a myriad of mechanisms including appropriate connections, cellular properties, and intrinsic circuitry, that facilitates its later selectivity. Future studies combining animal models with studies in other human populations, e.g. premature human infants, may help further elucidate these mechanisms.

A challenge of studying the functional organization of the neonatal brain is that there is no adequate way to localize functional responses using MRI in neonates. Here we

used functional regions from established studies and registered these regions to both adult and neonate brains using specialized software packages for infant image registrations. We also chose adjacent functional regions to test the spatial specificity of our findings. Future studies may consider new approaches to localize functional responses in young infants to further test the specificity of the current findings. Finally, we tested the Connectivity Hypothesis for the VWFA specifically. The findings suggest that connectivity-based scaffolding may be a general driving mechanism for the functional organization of human cortex, but the generality of this hypothesis for other mental domains remains to be tested.

References

1. Deen, B., *et al.* Organization of high-level visual cortex in human infants. *Nat Commun.* **8**, 13995 (2017).
2. van den Hurk, J., Van Baelen, M. & de Beeck, H.P.O. Development of visual category selectivity in ventral visual cortex does not require visual experience. *Proc Natl Acad Sci USA.* **114**, E4501-E4510 (2017).
3. Dehaene-Lambertz, G., Dehaene, S. & Hertz-Pannier, L. Functional neuroimaging of speech perception in infants. *Science.* **298**, 2013-2015 (2002).
4. Srihasam, K., Vincent, J.L. & Livingstone, M.S. Novel domain formation reveals proto-architecture in inferotemporal cortex. *Nat. Neurosci.* **17**, 1776 (2014).
5. Grill-Spector, K., Kourtzi, Z. & Kanwisher, N. The lateral occipital complex and its role in object recognition. *Vision research.* **41**, 1409-1422 (2001).

- 333 6. Dehaene, S. & Cohen, L. The unique role of the visual word form area in reading. *Trends*
334 *Cogn Sci.* **15**, 254-262 (2011).
- 335 7. Dehaene, S. & Cohen, L. Cultural recycling of cortical maps. *Neuron.* **56**, 384-398
336 (2007).
- 337 8. Osher, D.E., *et al.* Structural connectivity fingerprints predict cortical selectivity for
338 multiple visual categories across cortex. *Cereb. Cortex.* **26**, 1668-1683 (2015).
- 339 9. Saygin, Z.M., *et al.* Anatomical connectivity patterns predict face selectivity in the
340 fusiform gyrus. *Nat. Neurosci.* **15**, 321 (2012).
- 341 10. Osher, D.E., Brissenden, J.A. & Somers, D.C. Predicting an individual's Dorsal Attention
342 Network activity from functional connectivity fingerprints. *J. Neurophysiol.* (2019).
- 343 11. Tobyne, S.M., *et al.* Prediction of individualized task activation in sensory modality-
344 selective frontal cortex with 'connectome fingerprinting'. *Neuroimage.* **183**, 173-185 (2018).
- 345 12. Tavor, I., *et al.* Task-free MRI predicts individual differences in brain activity during task
346 performance. *Science.* **352**, 216-220 (2016).
- 347 13. Arcaro, M.J. & Livingstone, M.S. A hierarchical, retinotopic proto-organization of the
348 primate visual system at birth. *Elife.* **6**, e26196 (2017).
- 349 14. Baker, C.I., *et al.* Visual word processing and experiential origins of functional
350 selectivity in human extrastriate cortex. *Proc Natl Acad Sci U S A.* **104**, 9087-9092 (2007).
- 351 15. Dehaene, S., *et al.* How learning to read changes the cortical networks for vision and
352 language. *Science.* **330**, 1359-1364 (2010).
- 353 16. Malach, R., Levy, I. & Hasson, U. The topography of high-order human object areas. **6**,
354 176-184 (2002).

- 355 17. Hasson, U., Levy, I., Behrmann, M., Hendler, T. & Malach, R. Eccentricity bias as an
356 organizing principle for human high-order object areas. *Neuron*. **34**, 479-490 (2002).
- 357 18. Gomez, J., Barnett, M. & Grill-Spector, K. Extensive childhood experience with
358 Pokémon suggests eccentricity drives organization of visual cortex. *Hum Nat*. **1** (2019).
- 359 19. Bouhali, F., *et al.* Anatomical connections of the visual word form area. *J Neurosci*. **34**,
360 15402-15414 (2014).
- 361 20. Yeatman, J.D., Rauschecker, A.M. & Wandell, B.A. Anatomy of the visual word form
362 area: adjacent cortical circuits and long-range white matter connections. *Brain Lang*. **125**, 146-
363 155 (2013).
- 364 21. Epelbaum, S., *et al.* Pure alexia as a disconnection syndrome: new diffusion imaging
365 evidence for an old concept. *Cortex*. **44**, 962-974 (2008).
- 366 22. Saygin, Z.M., *et al.* Connectivity precedes function in the development of the visual word
367 form area. **19**, 1250 (2016).
- 368 23. Winkler, A.M., Ridgway, G.R., Webster, M.A., Smith, S.M. & Nichols, T.E.J.N.
369 Permutation inference for the general linear model. **92**, 381-397 (2014).
- 370 24. Sur, M., Garraghty, P.E. & Roe, A.W. Experimentally induced visual projections into
371 auditory thalamus and cortex. *Science*. **242**, 1437-1441 (1988).
- 372 25. Roe, A.W., Pallas, S.L., Hahm, J.-O. & Sur, M. A map of visual space induced in
373 primary auditory cortex. *Science*. **250**, 818-820 (1990).
- 374 26. Roe, A.W., Pallas, S.L., Kwon, Y.H. & Sur, M. Visual projections routed to the auditory
375 pathway in ferrets: receptive fields of visual neurons in primary auditory cortex. *J Neurosci*. **12**,
376 3651-3664 (1992).

- 377 27. Sharma, J., Angelucci, A. & Sur, M. Induction of visual orientation modules in auditory
378 cortex. *Nature*. **404**, 841 (2000).
- 379 28. Horng, S., *et al.* Differential gene expression in the developing lateral geniculate nucleus
380 and medial geniculate nucleus reveals novel roles for Zic4 and Foxp2 in visual and auditory
381 pathway development. *J Neurosci*. **29**, 13672-13683 (2009).
- 382 29. Stevens, W.D., Kravitz, D.J., Peng, C.S., Tessler, M.H. & Martin, A. Privileged
383 functional connectivity between the visual word form area and the language system. *J Neurosci*.
384 **37**, 5288-5297 (2017).
- 385 30. Dundas, E.M., Plaut, D.C. & Behrmann, M. The joint development of hemispheric
386 lateralization for words and faces. *J Exp Psychol Gen*. **142**, 348-358 (2013).
- 387 31. Augustine, E., Jones, S.S., Smith, L.B. & Longfield, E. Relations among early object
388 recognition skills: objects and letters. *Journal of Cognition and Development*. **16**, 221-235
389 (2015).
- 390 32. Kubota, E.C., Joo, S.J., Huber, E. & Yeatman, J.D. Word selectivity in high-level visual
391 cortex and reading skill. *Dev Cogn Neurosci*. (2018).
- 392 33. Makropoulos, A., *et al.* The developing human connectome project: A minimal
393 processing pipeline for neonatal cortical surface reconstruction. *Neuroimage*. **173**, 88-112
394 (2018).
- 395 34. Van Essen, D.C., *et al.* The WU-Minn human connectome project: an overview.
396 *Neuroimage*. **80**, 62-79 (2013).
- 397 35. Hughes, E.J., *et al.* A dedicated neonatal brain imaging system. *Magn Reson Med*. **78**,
398 794-804 (2017).

- 399 36. Makropoulos, A., *et al.* Automatic whole brain MRI segmentation of the developing
400 neonatal brain. **33**, 1818-1831 (2014).
- 401 37. Zollei, L., Ou, Y., Iglesias, J., Grant, P. & Fischl, B. FreeSurfer image processing
402 pipeline for infant clinical MRI images. *Hum Brain Mapp.* (2017).
- 403 38. de Macedo Rodrigues, K., *et al.* A FreeSurfer-compliant consistent manual segmentation
404 of infant brains spanning the 0-2 year age range. *Front Hum Neurosci.* **9**, 21 (2015).
- 405 39. Fitzgibbon, S.P., *et al.* The developing Human Connectome Project (dHCP): minimal
406 functional pre-processing pipeline for neonates. in *Fifth Biennial Conference on Resting State*
407 *and Brain Connectivity* (2016).
- 408 40. Salimi-Khorshidi, G., *et al.* Automatic denoising of functional MRI data: combining
409 independent component analysis and hierarchical fusion of classifiers. *Neuroimage.* **90**, 449-468
410 (2014).
- 411 41. Behzadi, Y., Restom, K., Liau, J. & Liu, T.T.J.N. A component based noise correction
412 method (CompCor) for BOLD and perfusion based fMRI. **37**, 90-101 (2007).
- 413 42. Glasser, M.F., *et al.* The minimal preprocessing pipelines for the Human Connectome
414 Project. *Neuroimage.* **80**, 105-124 (2013).
- 415 43. Fedorenko, E., Hsieh, P.-J., Nieto-Castañón, A., Whitfield-Gabrieli, S. & Kanwisher, N.
416 New method for fMRI investigations of language: defining ROIs functionally in individual
417 subjects. *J. Neurophysiol.* **104**, 1177-1194 (2010).
- 418 44. Desikan, R.S., *et al.* An automated labeling system for subdividing the human cerebral
419 cortex on MRI scans into gyral based regions of interest. **31**, 968-980 (2006).
- 420 45. Fedorenko, E., Duncan, J. & Kanwisher, N. Broad domain generality in focal regions of
421 frontal and parietal cortex. *Proc Natl Acad Sci USA.* **110**, 16616-16621 (2013).

- 422 46. Julian, J.B., Fedorenko, E., Webster, J. & Kanwisher, N. An algorithmic method for
423 functionally defining regions of interest in the ventral visual pathway. *Neuroimage*. **60**, 2357-
424 2364 (2012).
- 425 47. Pitcher, D., Dilks, D.D., Saxe, R.R., Triantafyllou, C. & Kanwisher, N. Differential
426 selectivity for dynamic versus static information in face-selective cortical regions. *Neuroimage*.
427 **56**, 2356-2363 (2011).
- 428 48. McCarthy, G., Puce, A., Gore, J.C. & Allison, T. Face-specific processing in the human
429 fusiform gyrus. *J Cogn Neurosci*. **9**, 605-610 (1997).
- 430 49. Kanwisher, N., McDermott, J. & Chun, M.M. The fusiform face area: a module in human
431 extrastriate cortex specialized for face perception. *J Neurosci*. **17**, 4302-4311 (1997).
- 432 50. Gauthier, I., *et al.* The fusiform “face area” is part of a network that processes faces at the
433 individual level. *J Cogn Neurosci*. **12**, 495-504 (2000).
- 434 51. Epstein, R. & Kanwisher, N. A cortical representation of the local visual environment.
435 *Nature*. **392**, 598-601 (1998).
- 436 52. Grill-Spector, K., *et al.* Differential processing of objects under various viewing
437 conditions in the human lateral occipital complex. *Neuron*. **24**, 187-203 (1999).
- 438 53. Frost, J.A., *et al.* Language processing is strongly left lateralized in both sexes: Evidence
439 from functional MRI. *Brain*. **122**, 199-208 (1999).
- 440 54. Wang, H. & Yushkevich, P. Multi-atlas segmentation with joint label fusion and
441 corrective learning—an open source implementation. *Front Neuroinform*. **7**, 27 (2013).
- 442 55. Menze, B.H., *et al.* The multimodal brain tumor image segmentation benchmark
443 (BRATS). *IEEE Trans Med Imaging*. **34**, 1993-2024 (2014).

56. Avants, B.B., *et al.* The Insight ToolKit image registration framework. *Front Neuroinform.* **8**, 44 (2014).

Online Methods

Participants.

Neonates. We used the initial release of the Developing Human Connectome Project (dHCP) neonatal data (<http://www.developingconnectome.org>)³³. Neonates were recruited and imaged at the Evelina Neonatal Imaging Centre, London. Informed parental consent was obtained for imaging and data release, and the study was approved by the UK Health Research Authority. 39 neonates were included in functional connectivity analysis and were born and imaged at term age (14 female, mean gestational age at birth = 39.03 weeks, gestational age range at scan = 37-44 weeks).

Adults. Adult data were obtained from the Human Connectome Project (HCP), WU-Minn HCP 1200 Subjects Data Release (<https://www.humanconnectome.org/study/hcp-young-adult>)³⁴. All participants were scanned at Washington University in St. Louis (WashU). 38 adults were included in functional connectivity analysis (19 female, age range = 22-36 years old).

Data acquisition.

463 *Neonates.*

464 Imaging was carried out on 3T Philips Achieva (running modified R3.2.2 software) using
465 a dedicated neonatal imaging system which included a neonatal 32 channel phased
466 array head coil³⁵. All neonates were scanned in natural sleep.

467 **Resting-state fMRI.** High temporal resolution fMRI developed for neonates using
468 multiband (MB) 9x accelerated echo-planar imaging was collected (TE/TR = 38/392ms,
469 voxel size = $2.15 \times 2.15 \times 2.15\text{mm}^3$). The duration of resting-state fMRI scanning was
470 approximately 15 minutes and consisted of 2300 volumes for each run. No in-plane
471 acceleration or partial Fourier was used. Single-band reference scans were also
472 acquired with bandwidth matched readout, along with additional spin-echo acquisitions
473 with both AP/PA fold-over encoding directions.

474 **Anatomical MRI.** High-resolution T2-weighted and inversion recovery T1-weighted
475 multi-slice fast spin-echo images were acquired with in-plane resolution $0.8 \times 0.8\text{mm}^2$
476 and 1.6mm slices overlapped by 0.8mm (T2-weighted: TE/TR = 156/12000ms; T1
477 weighted: TE/TR/TI = 8.7/4795/1740ms).

478 *Adults.*

479 All the scans of WU-Minn HCP 1200 Subjects Data Release was carried out using a
480 customized 3T Connectome Scanner adapted from a Siemens Skyra (Siemens AG,
481 Erlanger, Germany) with 32-channel Siemens receive head coil and a “body”
482 transmission coil designed by Siemens specifically for the smaller space available using
483 the special gradients for the WU-Minn and MGH-UCLA Connectome scanners.

Resting-state fMRI. Participants were scanned using the Gradient-echo EPI sequence (TE/TR = 33.1/720ms, flip angle = 52°, number of slices = 72, voxel size = 2 × 2 × 2 mm³). The duration of resting-state fMRI scanning was approximately 15 minutes and consisted of 1200 volumes for each run. All participants accomplished two resting-state fMRI sessions. Within each session, there were two phases encoding in a right-to-left (RL) direction in one run and phase encoding in a left-to-right (LR) direction in the other run. In current analysis, we used the LR phase encoding from the first session. Participants were instructed to open their eyes with relaxed fixation on a projected bright cross-hair on a dark background.

Anatomical MRI. High-resolution T2-weighted and T1-weighted images were acquired with isotropic voxel resolution of 0.7mm³ (T2-weighted 3D T2-SPACE scan: TE/TR = 565/3200ms; T1-weighted 3D MPRAGE: TE/TR/TI = 2.14/2400/1000ms)

Preprocessing.

Neonates.

The dHCP data were preprocessed using the dHCP minimal processing pipelines. For anatomical MRI data segmentation, the minimal preprocessing³³ included bias correction, brain extraction using BET from FSL, and segmentation of the T2w volume using DRAW-EM algorithm³⁶. In addition, a dedicated infant processing pipeline^{37, 38} in FreeSurfer v.6.0.0 (<http://surfer.nmr.mgh.harvard.edu/fswiki/infantFS>) was implemented to get a gray/white matter mask.

For resting-state fMRI data, the minimal preprocessing included the following steps³⁹: distortion-correction, motion correction, 2-stage registration of the MB-EPI functional image to T2 structural image and also generate combined transform from MB-EPI to 40-week T2 template, temporal high-pass filter (150s high-pass cutoff), and ICA denoising using FSL FIX⁴⁰. With the minimally preprocessed data, we additionally applied smoothing (Gaussian filter with the FWHM = 3 mm) within the all gray matter, and band-pass filter at 0.009-0.08 Hz. As a further denoising step, we used aCompCor⁴¹ to regress out signals from white matter and cerebrospinal fluid (CSF) to control the physiological noise like respiration and heartbeat as well as non-neuronal contributions to the resting state signal. All the FC analyses for the neonatal group were performed in native functional space.

Adults.

The HCP data were preprocessed using the HCP minimal preprocessing pipelines⁴². For anatomical data, a PreFreeSurfer pipeline was applied to correct gradient distortion, produce an undistorted “native” structural volume space for each participant by ACPC registration, extract the brain, perform a bias field correction, and register the T2-weighted scan to the T1-weighted scan. Each individual brain was also aligned to common MNI152 template (with 0.7mm isotropic resolution). Then, the FreeSurfer pipeline (based on FreeSurfer 5.3.0-HCP) was performed with a number of enhancements specifically designed to capitalize on HCP data⁴². The main goals of this pipeline are to segment the volume into predefined structures, reconstruct white and

pial cortical surfaces, and perform FreeSurfer's standard folding-based surface registration to their surface atlas (fsaverage).

For resting-state fMRI data, the minimal functional analysis pipelines included the following steps: removed spatial distortions, corrected for motion, registered the fMRI data to both structural and MNI152 template, reduced the bias field, normalized the 4D image to a global mean, and masked the data with the final brain mask. After, the data were further denoised using the novel ICA-FIX method⁴⁰. In order to preprocess these data in a pipeline that mirrored the neonatal group, we unwarped the data from MNI152 to native space, as the dHCP preprocessing pipeline did not perform this transformation. Just as the neonatal group, we then applied spatial smoothing (Gaussian filter with the FWHM = 3 mm) within all gray matter, band-pass filtered at 0.009-0.08 Hz, and implemented aCompCor.

Defining the functional parcels.

The VWFA parcel, located in left occipitotemporal cortex, was created from 20 adults (10 female, mean age = 24.6 years) by combining the 10% most responsive voxels in each adult that showed higher activation to words than line drawing objects²². The language parcels were released by Fedorenko et al. using a sentences vs. non-words contrast and created based on a probabilistic overlap map from 25 participants⁴³. We used seven key language parcels in left inferior frontal and left temporal cortex in the present study. We defined a speech parcel in superior temporal sulcus by overlapping

13 adults' speech ROIs (auditorily-presented English sentences vs. scrambled sentences contrast), and keeping the voxels where at least 6 of the 13 adults overlapped. We defined A1 using superior and transverse temporal cortex from the FreeSurfer Desikan-Killiany parcellation⁴⁴ in CVS average-35 MNI152 space. A set of multiple-demand (MD) parcels located in left frontal cortex were defined by higher response to a hard condition compared to an easy condition in a variety of cognitive tasks⁴⁵. High-level visual parcels used in the present study were derived from Julian et al.⁴⁶, which were identified based on a group of adults (n = 40) with a dynamic movie clips localizer⁴⁷. For the face selective parcels, FFA and OFA were identified with faces > objects contrasts⁴⁸⁻⁵⁰; for the scene selective parcel, PPA was identified with scenes > objects contrasts⁵¹; for the object selective parcels, LO and PFS were defined with objects > scrambled objects contrasts⁵². Because both VWFA and language are largely left lateralized^{30, 53}, our study includes left hemisphere seeds and targets only.

All functional parcels were originally in CVS average-35 MNI152 space, and were overlaid onto each individual's native anatomical brain using Advanced Normalization Tools (ANTs version 2.1.0; <http://stnava.github.io/ANTs>)⁵⁴⁻⁵⁶ for both adults and neonates. We further converted the parcels to native functional space using nearest neighbor interpolation with Freesurfer's mri_vol2vol function (https://surfer.nmr.mgh.harvard.edu/fswiki/mri_vol2vol).

To ensure no voxel belonged to more than one functional parcel, we assigned any intersecting voxels of two functional parcels to the one with smaller size. Additionally,

voxels within white matter and cerebellum were also removed. In total, we used 17 non-overlapping functional parcels from eight categories in the present study.

Calculating functional connectivity.

The mean timecourse of each functional parcel was computed from the preprocessed resting state images, and FC was calculated with Pearson's correlation between the mean timecourse of each seed parcel and each target parcel. To generate normally distributed values, each FC value was Fisher z-transformed.

FC fingerprint plots

First, we calculated the averaged FC from seed to each of the target category. Then we subtracted the mean FC across all categories from each of the averaged FC. Thus, the value in the fingerprint plots indicate how the seed connect to the target compared to the mean connections of seed to all categories.

Voxel-wise FC analysis in the ventral temporal cortex (VTC).

We performed a voxel-wise analysis across VTC to get a finer characterization of the connectivity pattern with language regions. We defined the VTC from the Desikan-Killiany parcellation⁴⁴, including the fusiform and inferior temporal labels, in FreeSurfer

587 CVS average-35 MNI152 space, which were registered to each individual's anatomy.
588 FC was computed between the mean timecourse of the language regions and the
589 timecourse of each VTC voxel. Without predefining any functional parcels within the
590 VTC, this analysis allowed us to characterize where the voxels with highest connectivity
591 were located within the VTC.

592 **Statistics.**

593 Within-subject design (i.e., repeated-measures) was used, in which case no
594 experimental group randomization or blinding in the present study. All *t* tests are paired
595 and two-tailed. The 95% confidence interval of the mean FC true population was also
596 reported for each *post hoc* paired *t* test. Data distribution was assumed to be normal,
597 but this was not formally tested.

598 **Data availability.** The data and codes that support the findings of this study are
599 available from the corresponding author upon request.